Supplement of Atmos. Chem. Phys., 20, 8421–8440, 2020
https://doi.org/10.5194/acp-20-8421-2020-supplement

Atmospheric Chemistry and Physics
Open Access
EGU

Supplement of

Chemical characterization of secondary organic aerosol at a rural site in the southeastern US: insights from simultaneous high-resolution time-of-flight aerosol mass spectrometer (HR-ToF-AMS) and FIGAERO chemical ionization mass spectrometer (CIMS) measurements

Yunle Chen et al.

Correspondence to: Nga L. Ng (ng@chbe.gatech.edu)

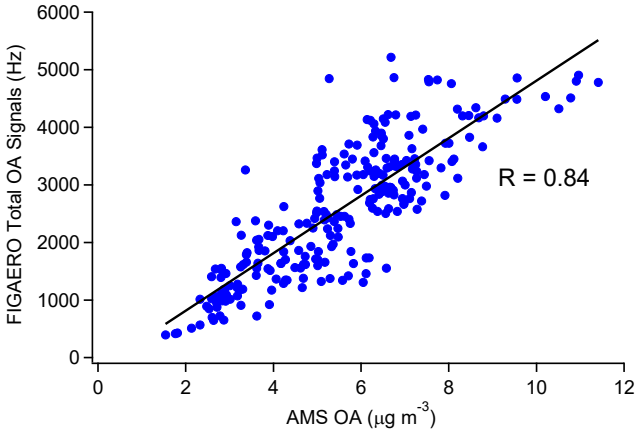

Figure S1 Correlation between FIGAERO total OA signals and AMS total OA mass concentration.

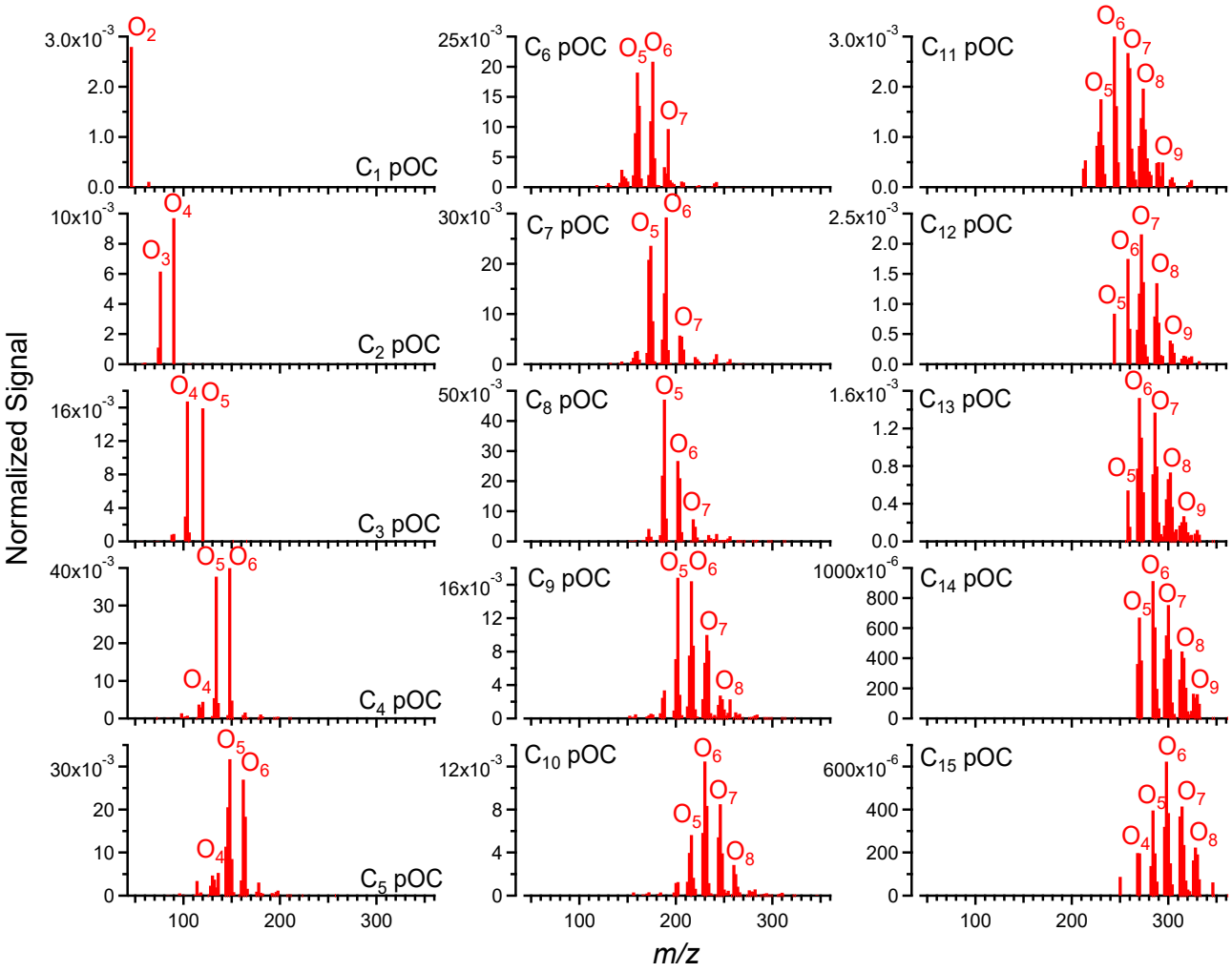

Figure S2 Normalized mass spectra of pOC ions measured by FIGAERO-CIMS, grouped by carbon atom number.

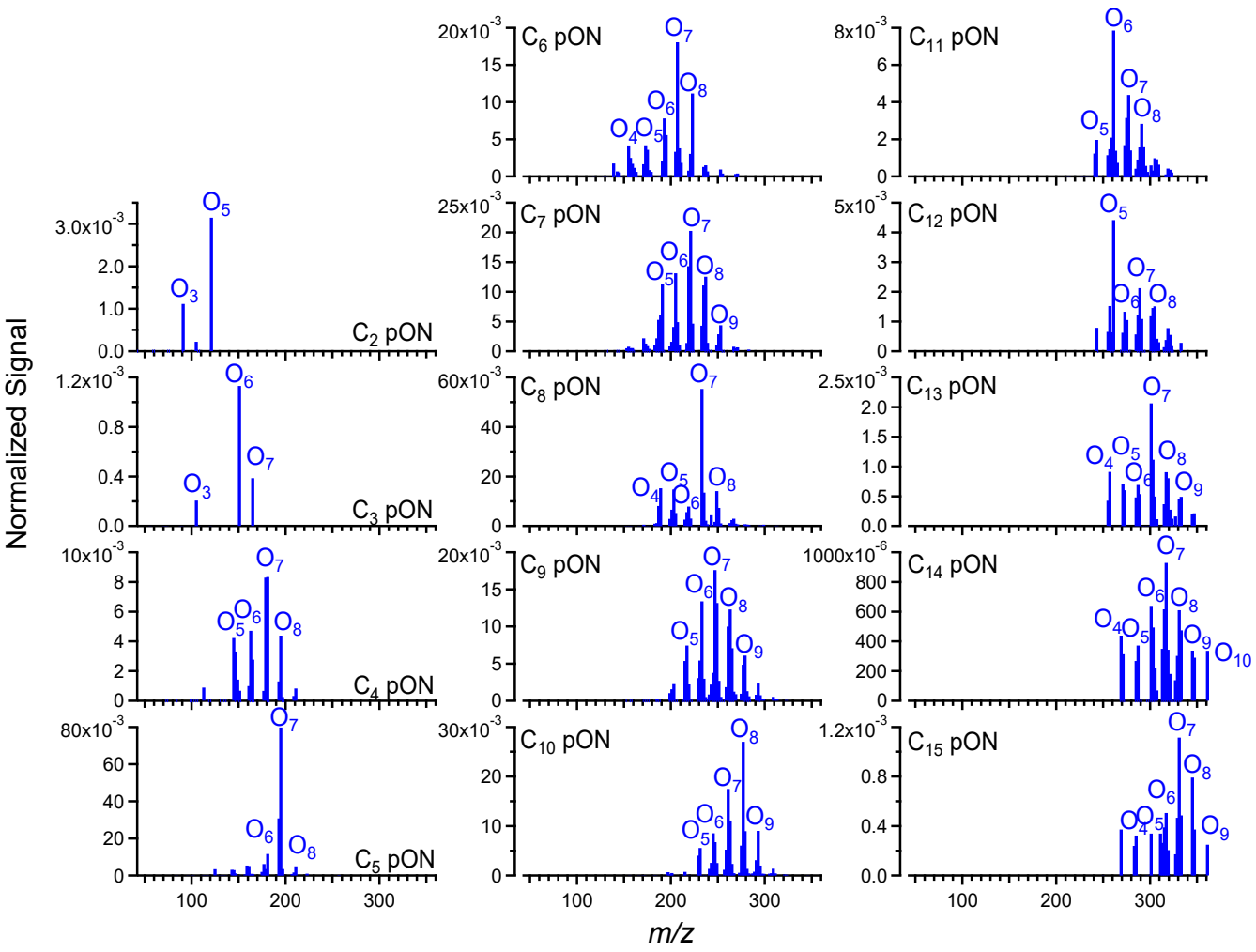

Figure S3 Normalized mass spectra of pON ions measured by FIGAERO-CIMS, grouped by carbon atom number.

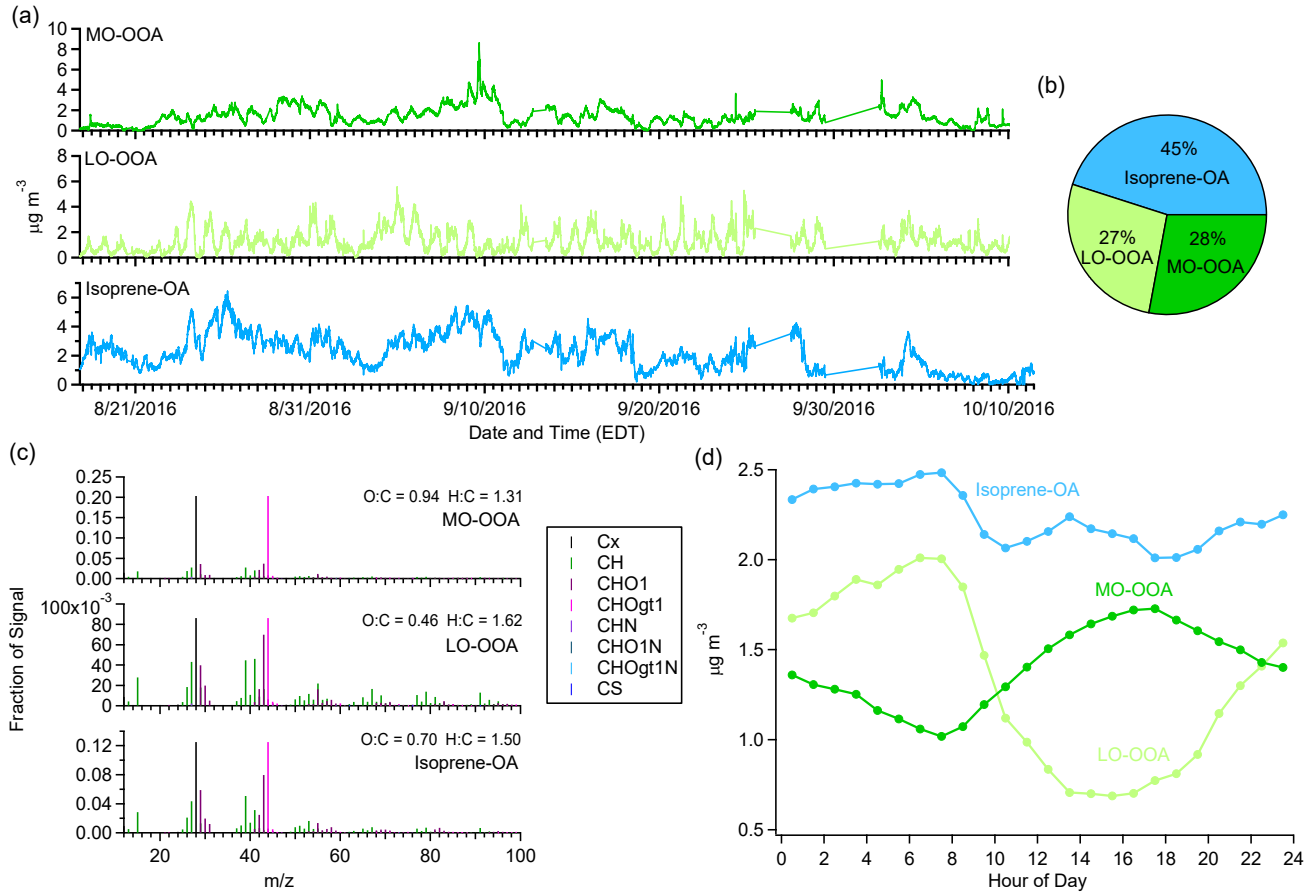

Figure S4 (a) Time series, (b) mass fraction, (c) normalized mass spectra, and (d) diurnal profiles of AMS OA factors resolved by PMF.

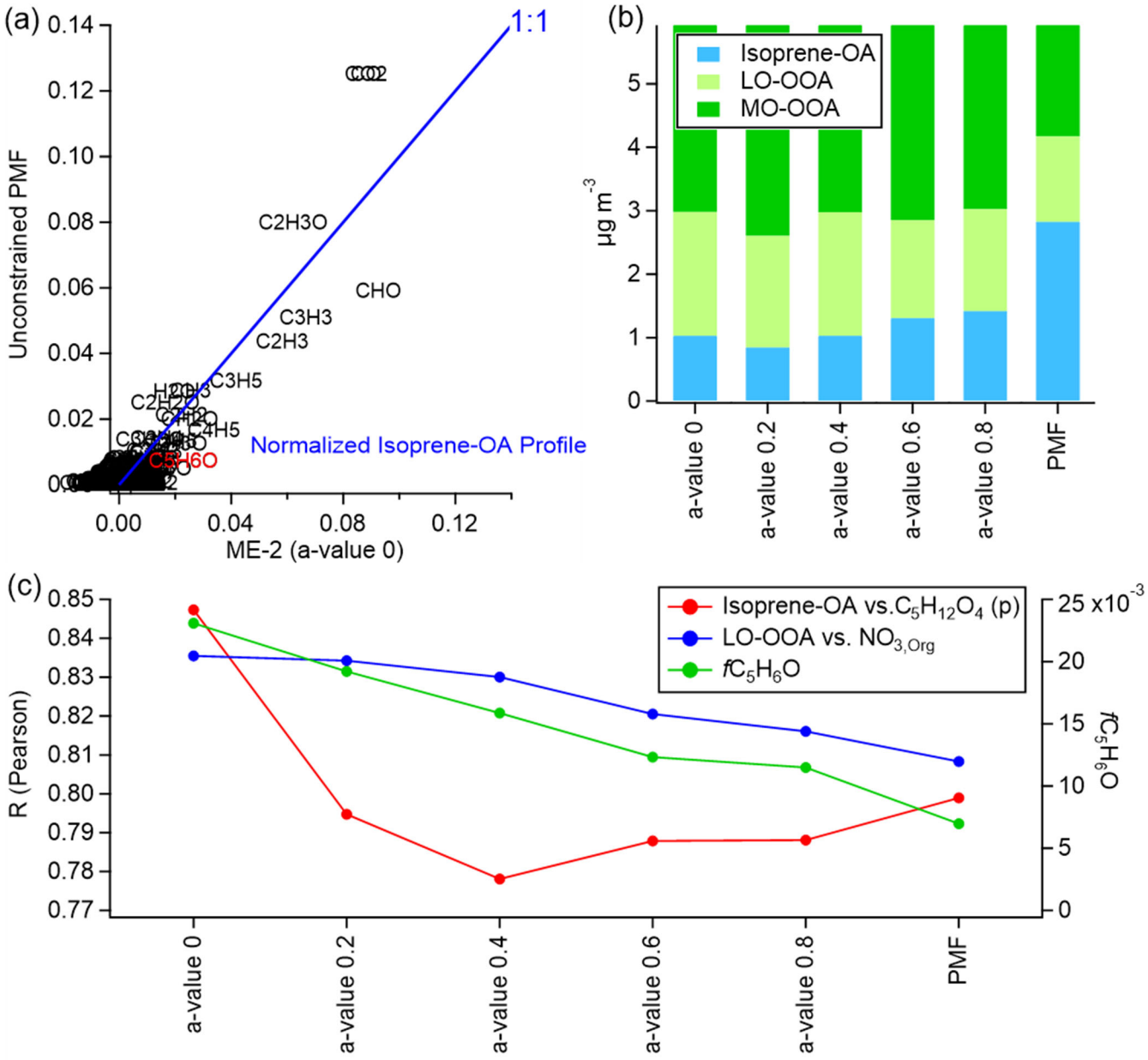

Figure S5 (a) comparison of Isoprene-OA profile resolved by PMF and ME-2 (a-value 0), (b) average mass concentration for the three factors for the model runs, and (c) correlations R (Pearson) between the time series of selected factors and the time series of tracers as a function of the model runs.

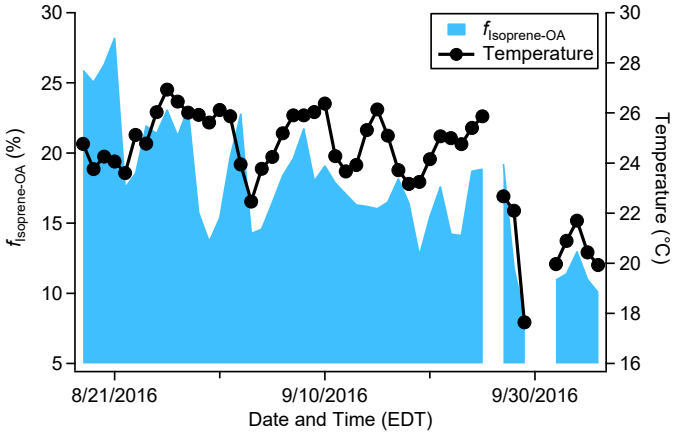

Figure S6 Time series (daily averaged) of the mass fraction of Isoprene-OA in total OA ($f_{Isoprene-OA}$) and temperature.

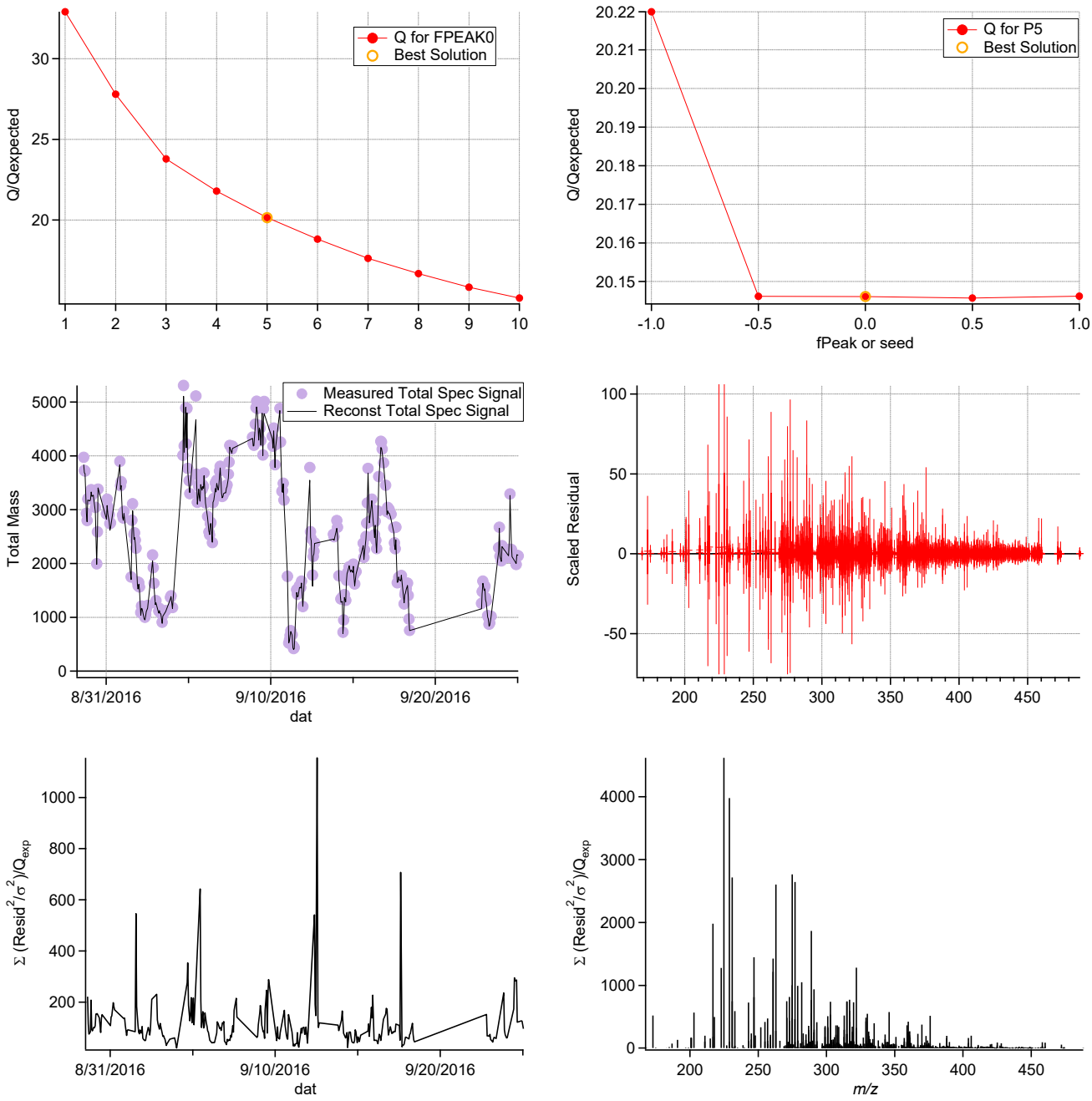

Figure S7 Diagnostic plots of PMF analysis on FIGAERO-CIMS measurements.

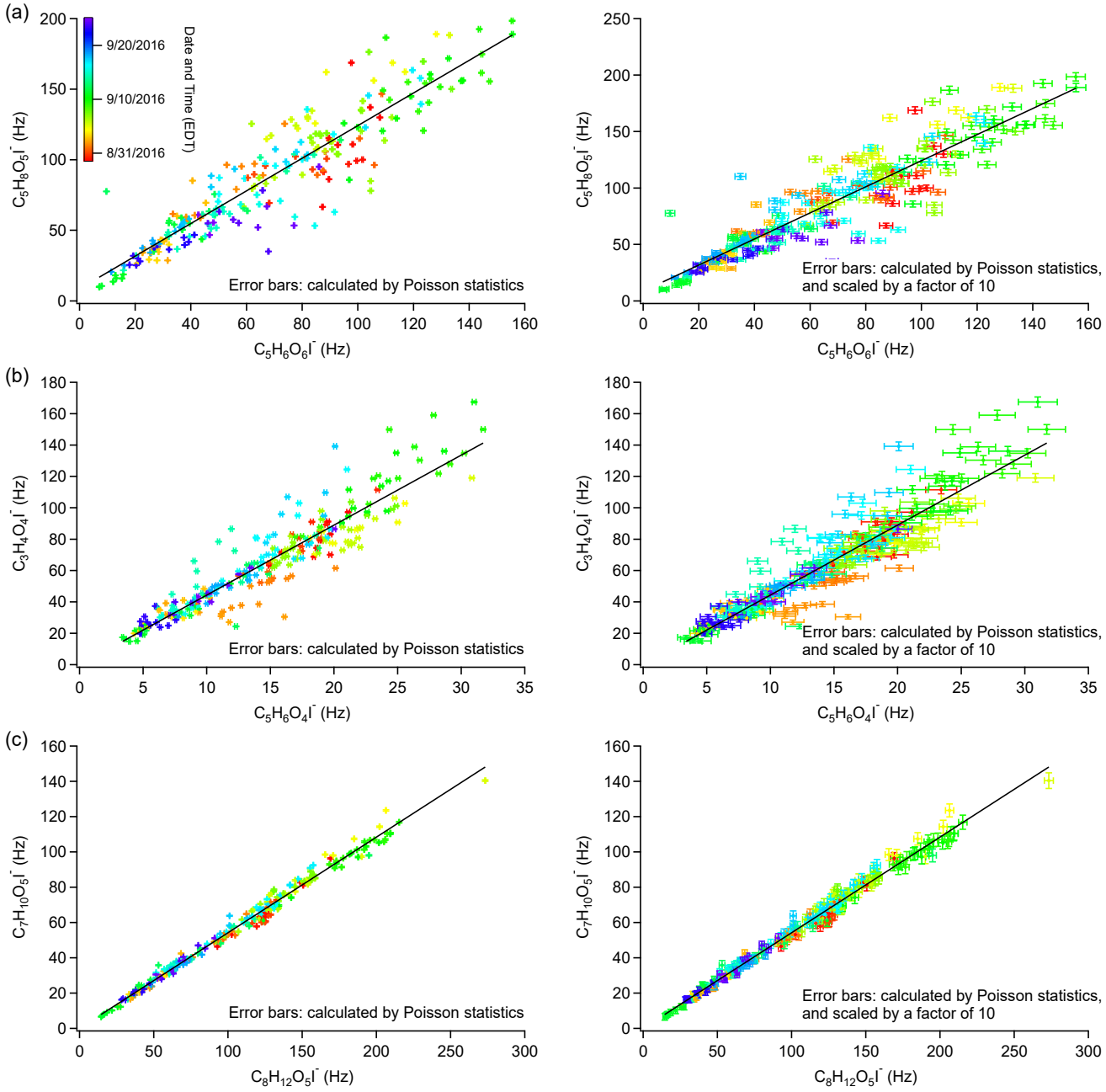

Figure S8 Scatter plots of pairs of highly-correlated ions, error bars representing estimated errors by simple Poisson statistics (left column) and after scaling by a factor of 10 (right column).

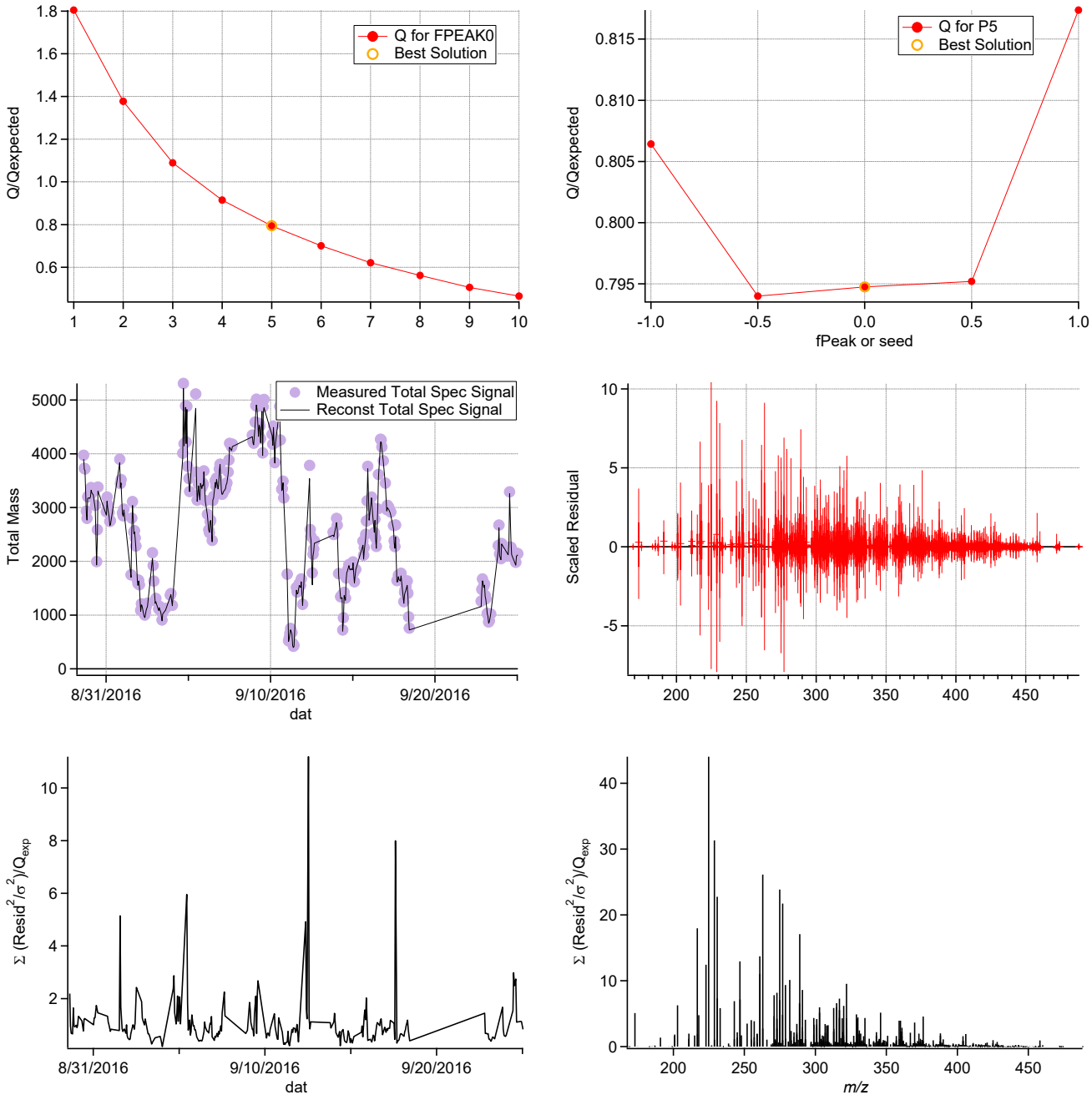

Figure S9 Diagnostic plots of PMF analysis on FIGAERO-CIMS measurements. Note that the input errors estimated from Poisson estimates were increased by a factor of 10 when performing PMF analysis.

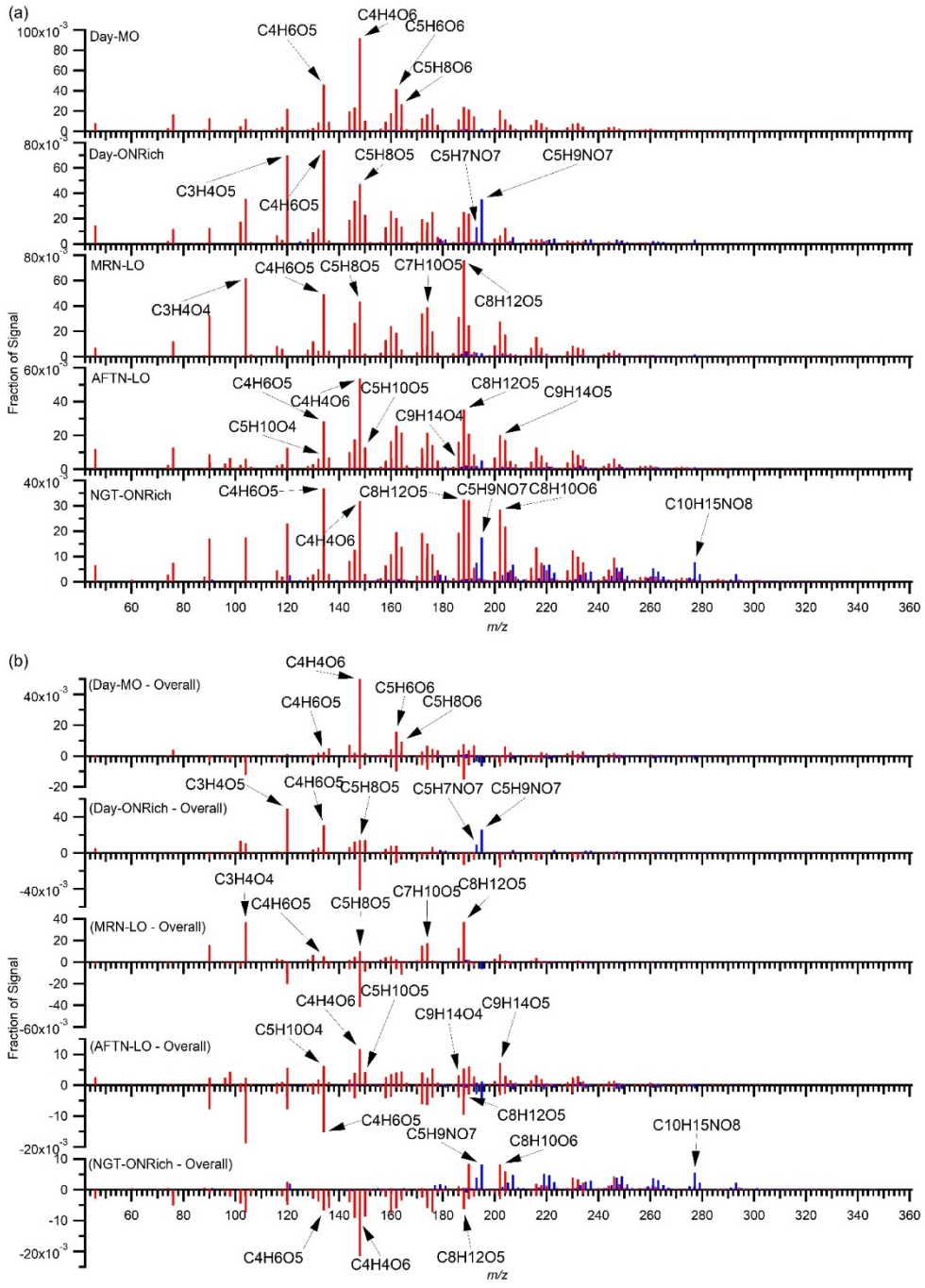

Figure S10 (a) normalized mass spectra of each FIGAERO OA factor and (b) difference between normalized mass spectra of each FIGAERO OA factor and normalized overall average mass spectra.

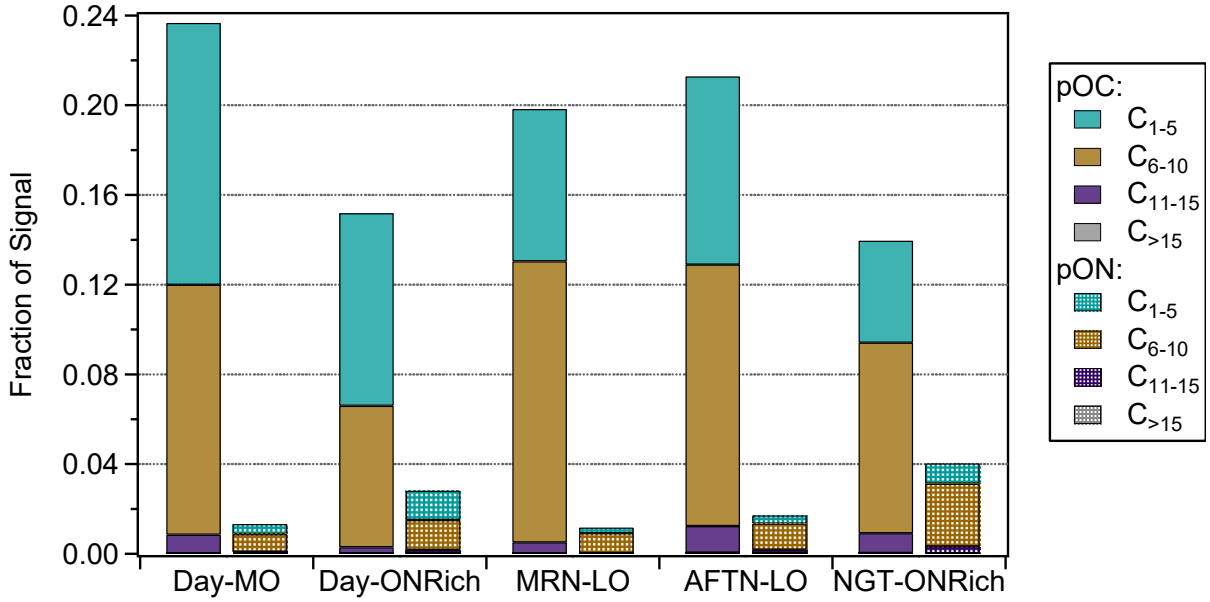

Figure S11 Fraction of pOC and pON ions of different carbon numbers (grouped as C1-5, C6-10, C11-15, and C>15) in total FIGAERO-CIMS signals.

5

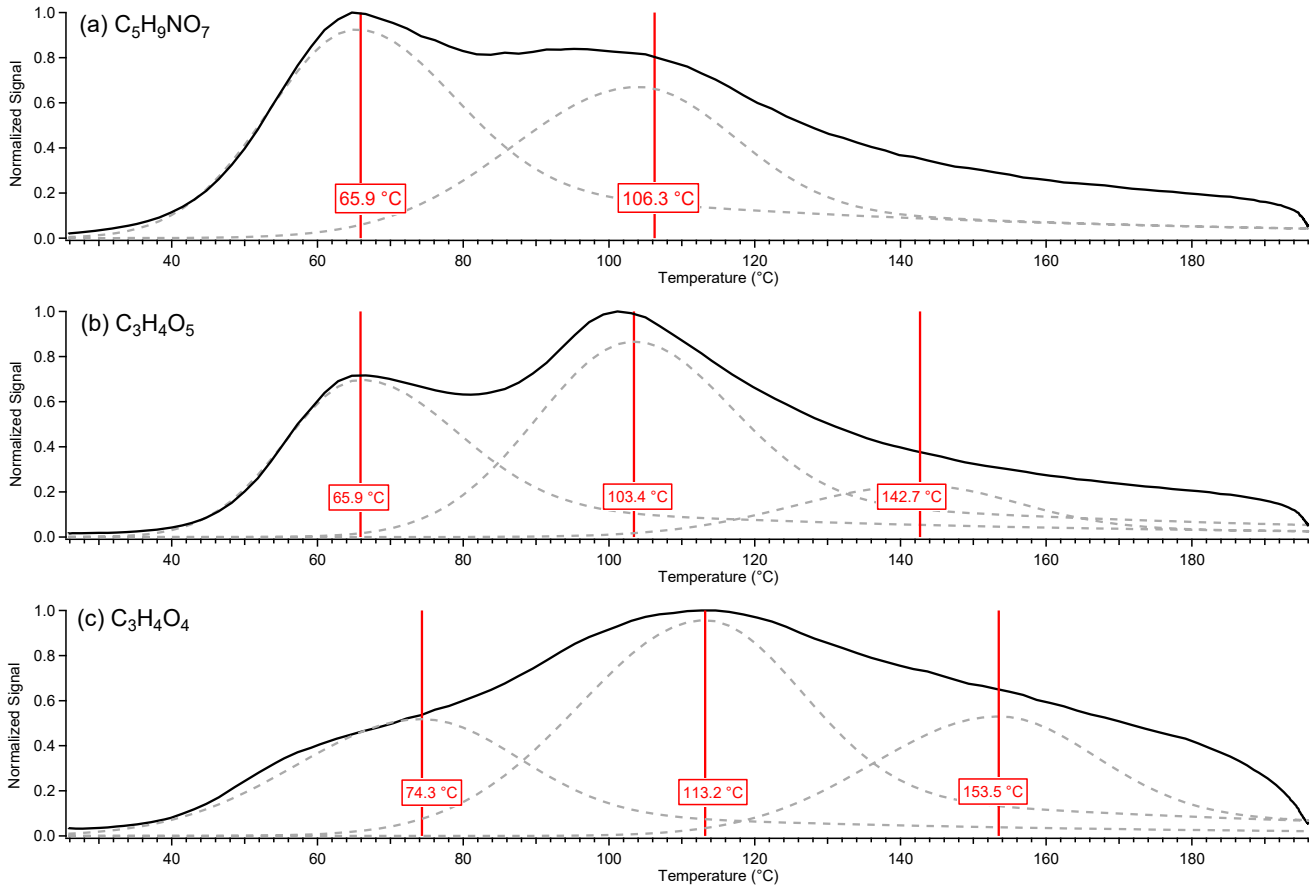

Figure S12 Thermograms of (a) $C_5H_9NO_7$, (b) $C_3H_4O_5$, and (c) $C_3H_4O_4$ ions measured by FIGAERO-CIMS.

Table S1 Most abundant 20 species of each FIGAERO factor listed in order of abundance.

	Day-MO	Day-ONRich	MRN-LO	AFTN-LO	NGT-LO
1	C4H4O6	C4H6O5	C8H12O5	C4H4O6	C4H6O5
2	C4H6O5	C3H4O5	C3H4O4	C5H8O5	C8H12O5
3	C5H6O6	C5H8O5	C4H6O5	C8H12O5	C7H10O6
4	C5H8O6	C3H4O4	C5H8O5	C4H6O5	C4H4O6
5	C5H8O5	C5H9NO7	C7H10O5	C5H6O6	C8H10O6
6	C8H12O5	C5H6O5	C7H8O5	C5H8O6	C3H4O5
7	C5H6O5	C6H8O5	C2H2O4	C7H10O5	C8H12O6
8	C6H8O6	C6H8O6	C8H10O5	C7H10O6	C5H6O6
9	C3H4O5	C8H12O5	C8H10O6	C9H14O5	C8H10O5
10	C7H10O6	C7H10O6	C5H6O5	C5H6O5	C7H8O5
11	C8H10O6	C5H10O5	C7H10O6	C8H12O6	C3H4O4
12	C5H4O5	C6H10O5	C6H8O5	C8H10O6	C5H9NO7
13	C7H8O6	C7H8O5	C6H8O6	C6H10O5	C2H2O4
14	C6H8O5	C5H4O5	C5H6O6	C6H8O5	C7H10O5
15	C2H4O3	C3H2O4	C9H14O5	C8H10O5	C5H8O6
16	C6H6O6	C7H10O5	C8H12O6	C6H8O6	C9H12O6
17	C6H8O7	C1H2O2	C6H10O5	C7H12O5	C5H6O5
18	C7H8O5	C5H6O6	C9H12O6	C5H10O5	C10H14O6
19	C2H2O4	C5H8O6	C7H8O6	C9H12O6	C7H8O6
20	C7H10O5	C5H7NO7	C6H6O5	C2H4O3	C5H8O5